Journal of Engineering Issues and Solutions

Fall Detection System for Elderly People Using LSTM

Sanim Kumar Khatri[1*], Devraj Parajuli[1], Prayag Man Mane[1], Bhupendra Chaulagain[1], Sandesh Thapa[1]

[1] Department of Electronics and Computer Engineering, Pulchowk Campus, Institute of Engineering, Nepal
**Corresponding email: khatri.sanim@gmail.com*
Received: November 25, 2025; Revised: 27 January, 2026; Accepted: March 21, 2026

Abstract

Falls are a leading cause of injury among older adults, requiring reliable real-time detection systems that can intervene promptly. This study proposes a detection system as a wearable device integrated with a six-axis Inertial Measurement Unit for sensing and a Raspberry Pi Pico microcontroller using a Long Short-Term Memory network for inference. Volunteers simulated elderly daily activities and fall cases to address practical constraints of real-world elderly data acquisition. The proposed double-layer LSTM architecture achieved an accuracy of 97.8%, compared to 92.19% obtained with the single-layer configuration, upon comparative evaluation, with corresponding reductions in false-positive and false-negative rates in confusion matrix analysis. The study highlights the potential of deep learning-based wearable technologies deployed on low-power hardware to improve elderly safety. The findings support the integration of wearable sensors and recurrent neural networks for monitoring and timely intervention for individuals with high chances and at high risk of falls. Future work could focus on the expansion of datasets, the integration of additional sensors, and testing in real-world environments.

Keywords: *Daily Activity Simulation, Elderly, Fall, IMU Sensor, LSTM, Wearables*

1. Introduction

Falls are among the leading causes of injuries and mortalities worldwide, with around 646,000 fatal incidents reported annually (World Health Organization, 2008). These incidents, often minor and preventable, pose significant risks of serious injuries, including fractures, head trauma, and even death, particularly among older adults (Long et al., 2022). A fall is a sudden, unintentional loss of balance that results in collapse to the ground, possibly caused by several factors, including but not limited to, health conditions like anemia and fluctuations in blood pressure, and hazards within the living environment. Delayed detection and extended periods of lying unattended can significantly increase the severity of complications and associated risks.

Automated fall detection systems offer a promising approach to mitigating fall consequences by enabling near-real-time intervention. The system uses simple sensors, such as an accelerometer and a gyroscope, as a wearable device to monitor movements and identify fall events. Unlike other methods, wearable devices

worn on the body allow continuous movement tracking and immediate detection of falls, eliminating delayed reporting or external observation (De Sario Velasquez et al., 2024). Enabling immediate alerts to caregivers or emergency services can ensure better safety and well-being for high-risk individuals, particularly older adults, both at home and in a healthcare environment, for timely medical intervention and improved quality of life. Thus, over the years, various hardware, techniques, and methods have been implemented to detect falls. Wearable devices equipped with accelerometers have gained attention due to their portability, real-time data processing, and reliability in detecting falls. Fall detection systems can be categorized into vision-based, ambient-based, wearable-based, machine learning (ML) and artificial intelligence (AI)-based, and hybrid system-based systems.

A fall detection system using a nine-axis IMU (with accelerometer, gyroscope, and magnetometer) was developed by Yan and Ou (2017) which was worn on the subject's waist. The system used quaternion Kalman filters to recognize the postures (Euler angles) and analyze the activity intensity, which helped to differentiate between lying and non-lying postures. In addition, the threshold method was used to detect falls. The system showed good accuracy in detecting inclined falls and posture recognition (lying and not lying postures). However, the statistical method had incorrect results when performing high-accelerometer activities such as running, jumping, as well as sitting down and standing up at a fast pace.

Bourke et al. (2010) evaluated twenty-one fall detection algorithms for continuous scripted and unscripted activities of a waist-mounted triaxial accelerometer. The study identified a novel algorithm with velocity, impact, and posture analysis threshold that achieves 100% specificity and sensitivity with a minimal false positive rate of 0.6 per day during continuous unscripted activities.

A fall detection system proposed by Badgujar and Pillai (2020) used a triaxial accelerometer positioned on the waist and analyzed data from the SisFall dataset (Sucerquia et al., 2017). The system utilized two machine learning algorithms, Support Vector Machines (SVM) and Decision Tree, to classify daily activities into fall and non-fall categories. Pre-processing involved a Butterworth filter to remove noise, and various features such as sum vector magnitude and standard deviation magnitude were extracted. The Decision Tree algorithm outperformed SVM, achieving an accuracy of 96%, with reduced false alarms compared to traditional threshold-based methods. However, the study mentions that accuracy could be further improved by expanding the training datasets and optimizing the feature selection process.

Mondal and Ghosal (2024) used data from accelerometer and gyroscope sensors and combined with an LSTM deep learning model and applied weight-turning to the LSTM model to enhance computational efficiency while maintaining performance. The model demonstrated high sensitivity and specificity, minimizing false negatives. However, the system relied on controlled environments for data collection, which limits its performance in real-world scenarios with a greater variety of activities.

Li et al. (2023) proposed a fall detection system for elderly individuals using multi-array, flexible, tactile sensors integrated into nursing aids. Sensors were strategically placed on the soles of these aids, targeting primary weight-bearing areas to capture plantar pressure data. The system employed their GCN-LSTM multi-task learning model to extract spatial and temporal features from the tactile data, enabling accurate prediction of future walking states and fall detection. Experiments demonstrated high accuracy (96.36%) for immediate fall detection and robust generalization across a variety of ground types and morphologies. However, performance slightly declined over longer prediction of horizons and on uneven surfaces such as slopes and stairs.

2. Materials and Methods

The robust elderly fall detection system was built using a viable wearable device consisting of an IMU sensor, a microprocessor, and a sophisticated LSTM network, a type of recurrent neural network (RNN) that can learn long-term dependencies between time steps in the data sequence (Hochreiter & Schmidhuber, 1997). The double layer LSTM model was used to analyze and detect fall events from the prepared dataset, which constitute the sequence of elderly motion activities and fall events. The 6-axis IMU sensor module was used to monitor the motion and movement of the subject (elderly people). It records the linear and angular acceleration of the body in real-time

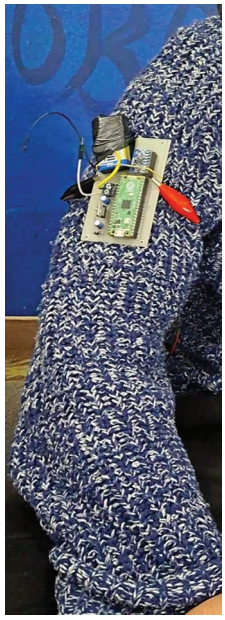

Figure 1: Wearable worn on the shoulder for stability.

situations and sends the sensor data to the microprocessor where it logs the data into the memory.

The sequence of motion information collected from the elderly was cleansed, and the wrangled data was used to train the LSTM model to detect fall events. The developed wearable device is shown in Figure 1.

The wearable device was developed to simultaneously monitor the motion activity of older adults and log the data recorded from the sensor in memory. MPU-6050, known for its reliability and precision, is a 6-axis IMU sensor module capable of measuring acceleration linearly in the range of up to ±16g, and angularly in the range of up to ±2,000 degrees per second.

The IMU sensor uses an Inter-Integrated Circuit(I2C) communication for data transmission with the RP2040 PI processor. It internally has three 16 bit analog/digital converters, for accelerometer and gyro sensors data discretization (Lage et al., 2016). The sensor is set to measure linear acceleration of up to ±4g and angular acceleration of up to ±500 degrees per second which was enough to capture motion and movement of the elderly.

The functional circuitry of the wearable device was designed in KICAD, a software suite for electronic circuit schematic capture and PCB design that offers open source and an active community (Vasetska, 2024). The circuit schematic and PCB layout of the viable wearable device are shown in Figure 2. The circuit is mainly sectioned into three parts on a single PCB board. The first section consists of a circuit for regulating the input DC voltage from an external source to provide a constant power supply to the microcontroller. The LM7805 IC voltage regulator was used to regulate an external source input voltage and to provide a constant 5V input to the microprocessor. The wearable device was required to connect to the computer to transfer and save sensor data previously logged in the microcontroller's memory. The microcontroller receives USB power when connected to computers. Two powers can be supplied in parallel to the microcontroller, one through a DC external source and the other from a USB power source. A Schottky diode is used in the Raspberry Pi Pico's input power because of its low forward voltage drop, which allows for efficient power delivery when using an external power source alongside the USB power, preventing back-feeding between the two sources while ensuring the

microcontroller always receives the highest available voltage. The diode prevents backflow current from parallel sources, safeguarding the internal power source from damage or unintentional charging. The second section of the PCB consists of a microprocessor and a wireless module connected to the microcontroller. The wireless module can be used to establish communication with the nearby alerting system to trigger alerts during events of falls. The IMU sensor is placed on the third section of the board.

The Raspberry Pi Pico, a low-cost, high-performance microcontroller board based on the RP2040 processor, was chosen due to its versatility, compact size, and ease of programming, which makes it suitable for IOT projects. It offers GPIO pins for peripheral interfacing and provides memory units for data storage. The microcontroller also took care of all the power supplies needed for its peripherals. The microcontroller was integrated with the MPU-6050 sensor to create a functional system for the wearable device.

The sequential movement and daily activities of older adults were captured and collected using the developed wearable device. To capture relevant movement data during fall, which typically last between 1 and 3 seconds (Yu, 2008), an observation time window of up to 8 seconds was considered around the peak of Subject Motion Variability (SMV) (4 seconds before and after the peak). These measurements (representing mobility patterns during the fall) are then used as input to the fall detection algorithm (Medrano et al., 2014) (Igual et al., 2015) (Micucci et al., 2017). The motion patterns of elderly people were researched and observed to ensure accurate data collection. Using actual elderly individuals to participate in the data collection is nearly impossible as capturing the fall events of individuals requires the individual to fall on the ground. Fall events do not play an important role in distinguishing the fall patterns of various age groups. The significant pattern difference is seen in other day-to-day movement activities such as walking, leaning down, sitting, and standing among various age groups. Even among the elderly, movement patterns vary significantly.

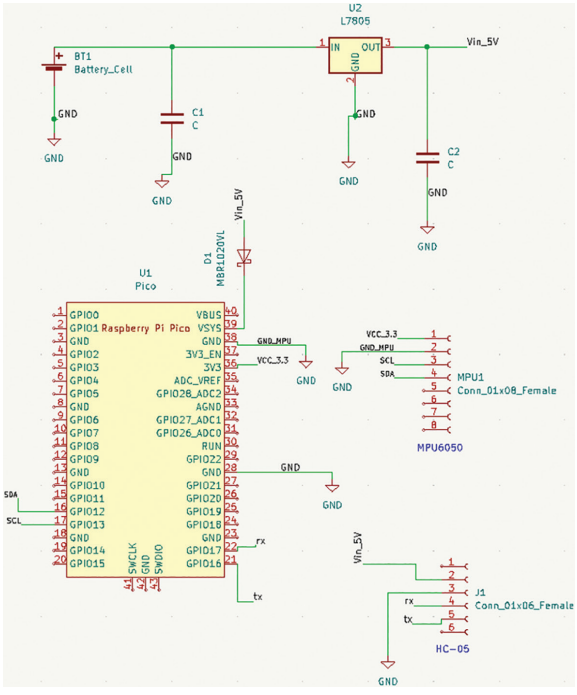

2(a). Schematic circuit of wearable device.

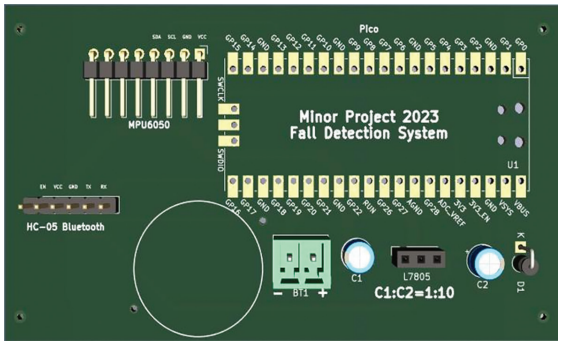

2(b). KICAD PCB Layout for wearable.

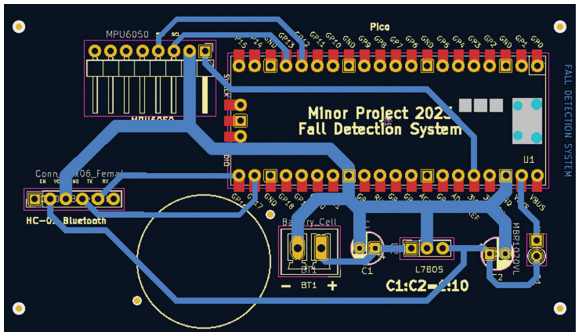

2(c). PCB layout 3D view of wearable.

Figure 2: Wearable device functional circuitry schematic and PCB layout

A study had been conducted to study and characterize the movement patterns of older individuals with T2D in free-living environments (Yahalom-Peri et al., 2023). The study concluded significant differences in movement patterns among elderly people and suggested that analysis of movement patterns can be useful in segregating individuals who are most likely to fall or are at high risk due to falls. To create daily movement patterns in the elderly to improve the accuracy of the proposed LSTM model, various day-to-day movement activities of the elderly are mimicked during data collection.

Similarly, the impact of unwanted motion on the wearable was also minimized by wearing it on certain parts of the body. Unwanted body motion on wearable devices can affect accuracy and lead to false positive or true negative in fall detection. Motion impedance of the human body can lead to misleading results of fall detection systems. It must be worn in such places on the body where there is the least effect of human motion impedance, and the device is relatively stable. The body map of Figure 3 shows the best places to put wearable devices on the body, where they will be the least obtrusive and cause the least amount of body motion impedance (Zeagler, 2017).

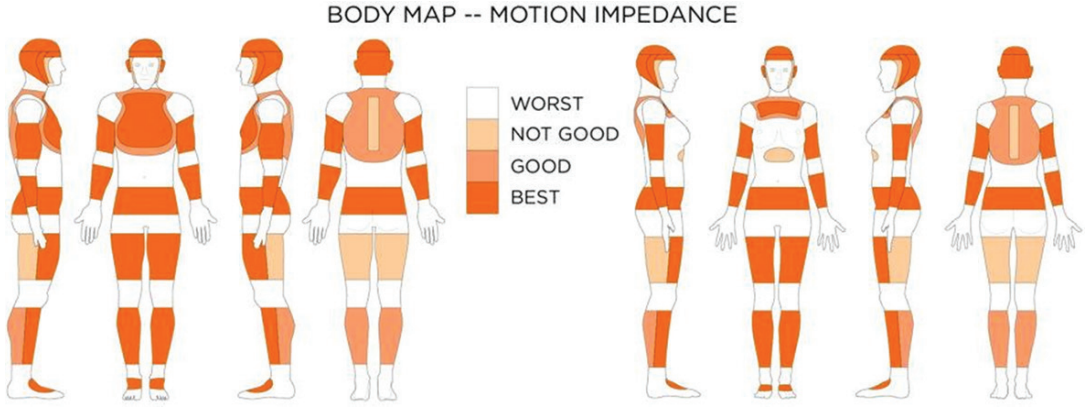

Figure 3: The best and worst part of the body to wear the wearable by considering the effect of motion impedance on the device (Zeagler, 2017).

3. Results and Discussion

Before feeding the prepared data set into LSTM to detect fall events, the data set was visualized to analyze and observe motion and activity patterns. The graph in Figure 4 shows the acceleration variations during different day-to-day motion activities, including fall events, providing a clear distinction between day-to-day motion activities and fall events.

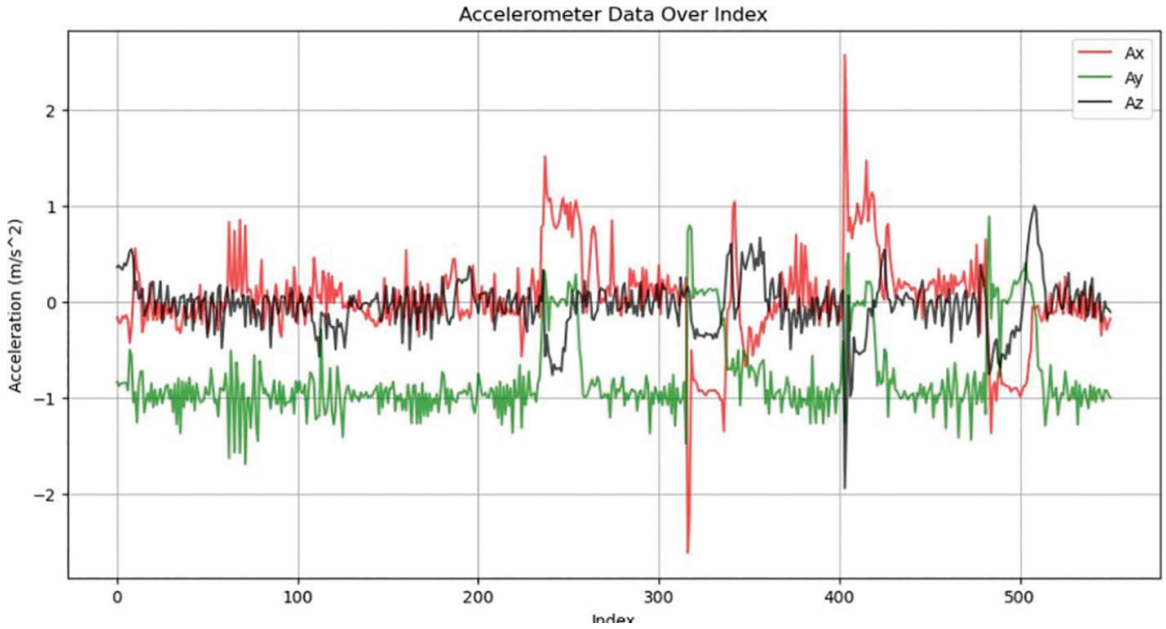

Figure 4: Graph representing accelerometer data for different activities for person 1.

Sudden spikes are seen due to the sudden increase in acceleration data, indicating fall events, which are different from flat or consistent patterns that represent other data such as standing, running, and walking. Similarly, Figure 5 demonstrates the variations in the angular velocity. Sudden spikes in the graph are seen as a result of an instantaneous change in the angular velocity, denoting the occurrence of the fall.

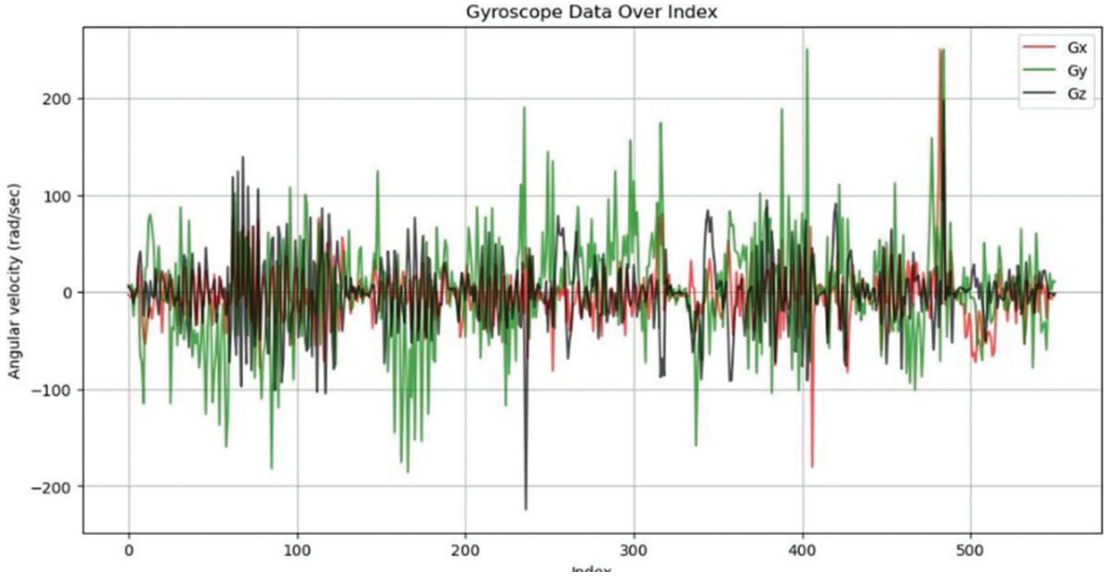

Figure 5: Graph representing gyroscope data for different activities for person 1.

To visualize accelerometer data and gyroscope data in a single graph, the data were scaled in specific ranges. After numerous experimental trials and observations, the optimal range for accelerometer data and gyroscope data for effective visualization was determined to be [-10, 10] and [-20, 20], respectively. Scaling the data in the range helped in effective visualization of the fall and non-fall data. The scaled data were plotted together on the same graph, and the highest values were observed to distinguish the fall datasets from the non-fall as shown in Figure 6 and the interval represented with the shaded region on the graph denotes the fall dataset. Falls can be associated with peaks in acceleration data that originate due to abrupt changes in reading when the body hits the ground (Hsieh et al., 2017).

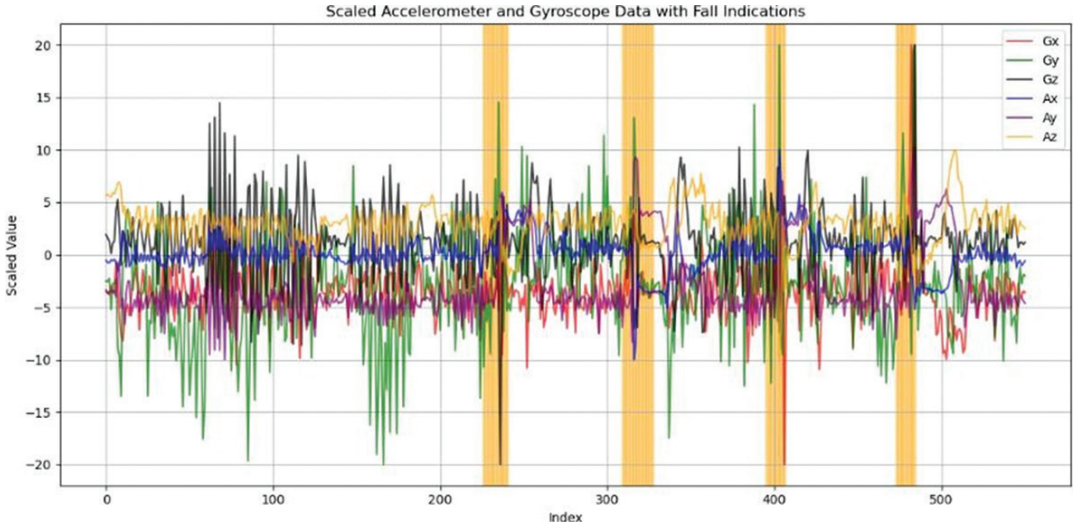

Figure 6: Graph representing fall and no fall data for person 1.

Initially, the single-layer LSTM model with 32 hidden units capable of capturing temporal dependencies in sequential data was used. A dropout layer was introduced to mitigate overfitting. The model achieved an accuracy of 92.20%. The architecture of the model is illustrated in Table1.

Table 1: Single-Layer LSTM Model Summary Table

Layer (type)	Output Shape	Param #
lstm (LSTM)	(None, 32)	4,992
dropout (Dropout)	(None, 32)	0
dense (Dense)	(None, 16)	528
dense_1(Dense)	(None, 1)	17

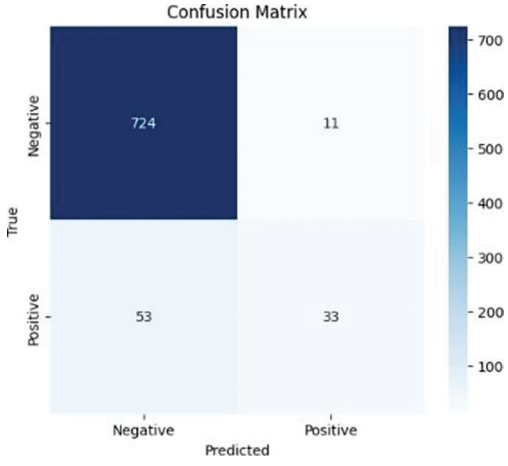

Figure 7: Confusion matrix obtained from a 1-layer LSTM model.

The confusion matrix for the single-layer LSTM model is shown in Figure 7. From the confusion matrix, it is evident that, although 724 out of 735 non-fall data points were correctly identified as non-fall, the model struggled to accurately classify the fall data. Moreover, only 33 of the 86 data points were accurately identified. Although the model showed high overall accuracy (of more than 92%), its performance in detecting fall events was significantly lower. Given the project's primary objective of detecting fall scenarios to mitigate their consequences, this model's limited ability to accurately identify falls rendered it unsuitable for the intended application despite its high accuracy.

To minimize the calibration gap given by the single-layered LSTM model, a second LSTM model was designed, which incorporated two LSTM layers with 64 and 32 hidden units, respectively. A dropout layer was introduced after each LSTM layer to mitigate overfitting. The double-layered LSTM model achieved a high accuracy of 97.80% and its architecture is illustrated by Table 2.

Table 2: 2-layer LSTM Model Summary Table

Layer (type)	Output Shape	Param #
Negative	(None, 100, 64)	18,176
Positive	(None, 100, 64)	0
lstm_1 (LSTM)	(None, 32)	12,416
dropout_1 (Dropout)	(None, 32)	0
dense (Dense)	(None, 32)	1,056
dense_1 (Dense)	(None, 1)	33

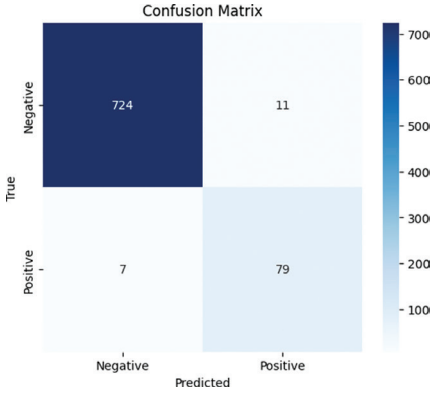

Figure 8: Confusion matrix obtained from a 2-layer LSTM model.

Data were trained in both layers with the same batch size of 32. Adam optimizer with its default learning rate of 0.001 was used. The training was set to run for 25 epochs for both models. Although the single-layered LSTM model was trained for full 25 epochs, the double-layer model stopped early at epoch 19 as the validation loss had stabilized and showed no further improvement beyond the point. By stopping the training process at an optimal point, the model was ensured to not memorize the training data, prevent overfitting, and suggest improved generalization.

The inaccuracy obtained in the single-layer LSTM model was significantly reduced with the improved architecture of the double-layered LSTM model. As shown in Figure 8, with the same number of test data, the double-layered LSTM model correctly classified 79 of the 86-fall events data, resulting in an increase in fall detection recall from below 40% to above 90%. Concurrently, the model maintained its high accuracy in classifying the non-fall data, demonstrating a significant improvement in overall fall detection reliability compared to the single-layer LSTM model.

Furthermore, evaluation metrics were compared to analyze the classification performance of the designed single-layer LSTM model and the double-layer LSTM model as shown in Table 3, where the double-layer LSTM model demonstrated superior performance compared to a single-layer LSTM model.

Table 3: Model Performance Comparison of 1-layer and 2-layer LSTM model

Model	ACC (%)	SEN (%)	PREC. (%)	F1-Score (%)
1-Layer LSTM	92.19	38.37	75.00	50.77
2-Layer LSTM	97.8	91.86	87.78	89.77

In terms of fall detection, the double-layered LSTM model showed a significant improvement. Although the single-layer model struggled to detect fall events achieving a precision of 75.00%, a sensitivity of 38.37%, and an F1 score of 50.77%, the double-layered LSTM effectively detected fall events, raising the precision to 87.78%, sensitivity to 91.86%, and F1 score to 89.77%.

To further analyze the training process and performance of both models, the training and validation loss and accuracy plots of both models were compared in Figure 9 and Figure 10.

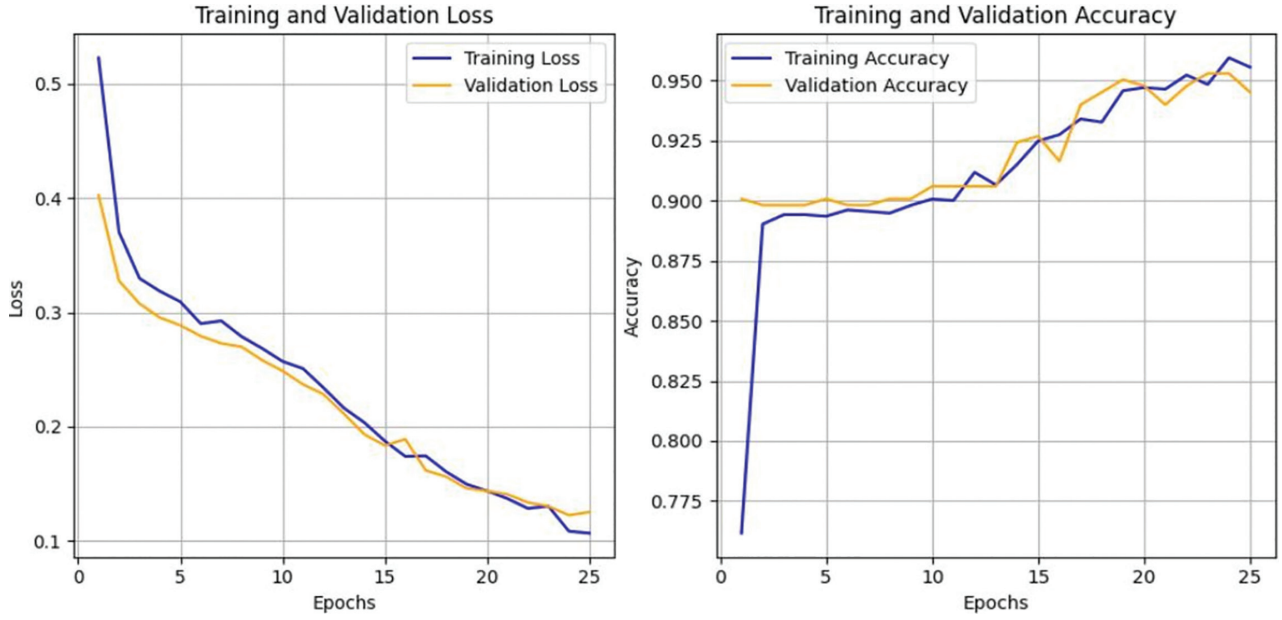

9(a). Training and Validation Loss9 9(b). Training and Validation Accuracy

Figure 9: Training and Validation Loss and Accuracy from 1-layer LSTM model.

Figure 9(a) shows that the training loss of a single-layered LSTM model decreased steadily, indicating that the model continued to minimize the error in the training set. However, the validation loss initially decreased and fluctuated slightly in later epochs. Similarly, Figure 9(b) shows that the single layered model's training accuracy rose consistently, indicating that the model was effectively optimizing its parameter during training. However, the validation accuracy plateaued around 94%, suggesting that the model reached its generalization early. These observations, like fluctuations in validation loss and plateau in validation accuracy, suggested that the single-layered model has limited capacity to generalize further and might start overfitting after certain epochs.

Figs. 10(a) and 10(b) demonstrate different behaviors. In Figure 10(a), the training loss decreased steadily in earlier epochs and reached a minimal value, indicating an effective optimization.

The validation loss also decreased steadily and without significant fluctuations, indicating stability and stronger generalization. In Figure 10(b), the training accuracy increased rapidly during the initial epochs, converging near 100%, while the validation accuracy increased rapidly during the initial epochs and stabilized at around 97%. This close alignment between two curves suggests that this model generalizes well to unseen data.

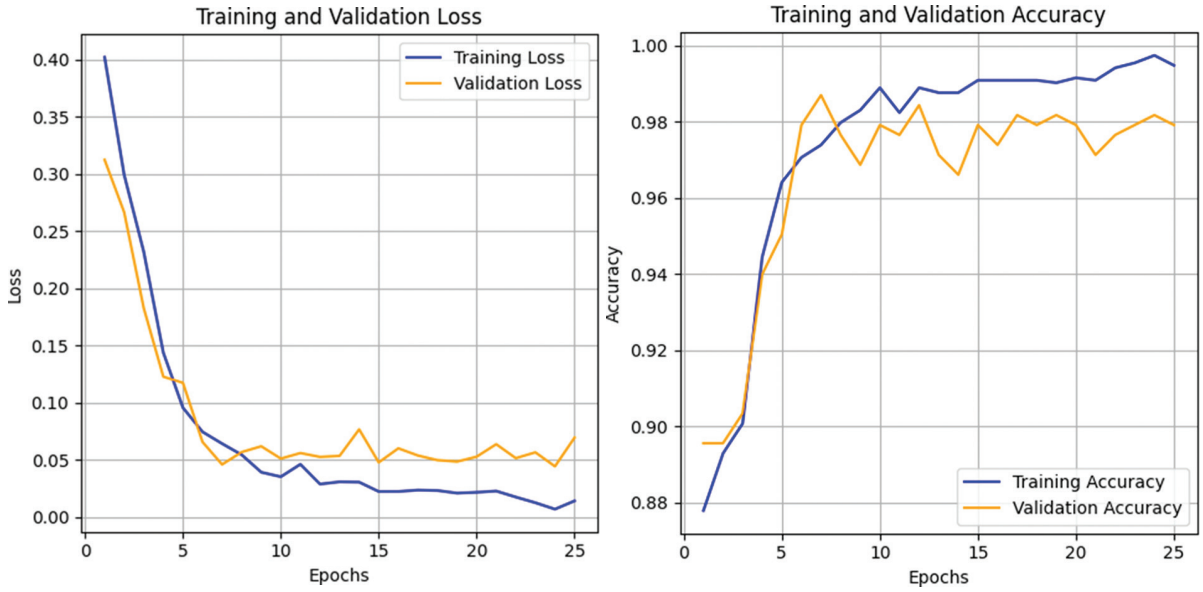

10(a). Training and Validation Loss 10(b). Training and Validation Accuracy

Figure 10: Training and Validation Loss and Accuracy from 2-layer LSTM model.

The double-layered model exhibited lesser loss and higher accuracy as indicated by Figure 9 and Figure 10. These observations suggest that the double-layered model effectively captures temporal dependencies and complex patterns within the data, leading to superior performance and better generalization.

The single-layer model, despite demonstrating ability to process sequential data well, performed poorly in the designated task of detecting fall events. The reason behind this was improper temporal representation, as fall detection requires discerning uncommon patterns like transitions from standing to falling, or from running to falling, which single-layered model struggles to represent properly due its inability to handle long-term dependencies and temporal transitions. However, double-layer LSTM facilitates hierarchical learning of temporal features. The first layer captures lower-level patterns like changes in acceleration or angular velocity, while the second layer refines these features into higher-level abstractions, enhancing the model's ability to detect falls despite varied movements. Along with this, the detection process suffers from class imbalance, as non-fall activities are higher in number than fall activities. As a result, single layer LSTM is biased toward the majority class, thus resulting in poor sensitivity to fall activities. However, the double layered model was able to learn more informative characteristics from samples from the minority class, making it more sensitive to fall incidents, thus exhibiting superior overall performance.

4. Conclusion

This study presents a sensor-integrated wearable fall detection system with an LSTM-based model to detect fall incidents in high-risk older adults. Critical challenges in data collection are addressed by simulating

typical regular activities of the elderly. The proposed system achieved an accuracy of 97.60%. The findings demonstrate the potential of wearable technology with machine learning to improve fall detection and enhance safety and well-being. Future work could focus on expanding the datasets to include diverse populations, validating the system in real-world environments, and incorporating additional sensors.

References

Badgujar, S., & Pillai, A. S. (2020). Fall detection for elderly people using machine learning. 11th International Conference on Computing, Communication and Networking Technologies(ICCCNT),1–7. https://doi.org/10.1109/ICCCNT49239.2020.9225494

Bourke, A. K., van de Ven, P., Gamble, M., O'Connor, R., Murphy, K., Bogan, E., McQuade, E., Finucane, P., ÓLaighin, G., & Nelson, J. (2010). Evaluation of waist-mounted tri- axial accelerometer-based fall-detection algorithms during scripted and continuous unscripted activities. Journal of Biomechanics, 43(16), 3051–3057. https://doi.org/10.1016/j.jbiomech.2010.07.005

De Sario Velasquez, G. D., Borna, S., Maniaci, M. J., Coffey, J. D., Haider, C. R., Demaerschalk, B. M., & Forte, A. J. (2024). Economic perspective of the use of wearables in health care: A systematic review. Mayo Clinic Proceedings: Digital Health, 2(3), 299–317. https://doi.org/ 10.1016/j.mcpdig.2024.05.003

Hochreiter, S., & Schmidhuber, J. (1997). Long short-term memory. Neural Computation, 9(8), 17351780. https://doi.org/10.1162/neco.1997.9.8.1735

Hsieh, C.-Y., Liu, K.-C., Huang, C.-N., Chu, W.-C., & Chan, C.-T. (2017). Novel hierarchical fall detection algorithm using a multiphase fall model. Sensors, 17(2), 307. https://doi.org/10.3390/s17020307

Igual, R., Medrano, C., & Plaza, I. (2015). A comparison of public datasets for acceleration- based fall detection. Medical engineering & physics, 37(9), 870–878. https://doi.org/doi:10.1016/j.medengphy.2015.06.009

Lage, V. N., Rêgo Segundo, A. K., & Barsante e Pinto, T. V. (2016). Mathematical modelling of a two degree of freedom platform using accelerometers and gyro sensors. Journal of Mechanics Engineering and Automation, 6, 427–433. https://doi.org/10.17265/2159-5275/2016.08.006

Li, T., Yan, Y., Yin, M., An, J., Chen, G., Wang, Y., Liu, C., & Xue, N. (2023). Elderly fall detection based on GCN-LSTM multi-task learning using nursing aids integrated with multi-array flexible tactile sensors. Biosensors (Basel), 13(9). https://doi.org/10.3390/bios13090862

Long, S., Hu, L., Luo, Y., Li, Y., & Ding, F. (2022). Incidence and risk factors of falls in older adults after discharge: A prospective study. Int J Nurs Sci, 10(1), 23–29. https://doi.org/10.1016/j. ijnss.2022.12.010

Medrano, C., Igual, R., Plaza, I., & Castro, M. (2014). Detecting falls as novelties in acceleration patterns acquired with smartphones. PloS one, 9(4), e94811. https://doi.org/10.1371/journal. pone.0094811

Micucci, D., Mobilio, M., Napoletano, P., & Tisato, F. (2017). Falls as anomalies? an experimental evaluation using smartphone accelerometer data. Journal of Ambient Intelligence and Humanized Computing, 8, 87–99. https://doi.org/10.48550/arXiv.1507.01206

Mondal, R., & Ghosal, P. (2024). Recall-driven precision refinement: Unveiling accurate fall detection using lstm. In D. Puthal, S. Mohanty, & B.-Y. Choi (Eds.), Internet of things. advances in information and communication technology (pp. 74–83). Springer Nature Switzerland. https://doi.org/10.1007/978-3-031-45882-8_6

Sucerquia, A., Lopez, J., & Vargas-Bonilla, J. (2017). Sisfall: A fall and movement dataset. Sensors, 17, 198. https://doi.org/10.3390/s17010198

Vasetska, L. (2024). A study of the electric circuit modelling and simulation software efficiency and their accuracy, speed and ease of use comparison., 29, 32–44. https://doi.org/10.62660/bcstu/ 2.2024.32

World Health Organization. (2008). Who global report on falls prevention in older age [47 pages]. https://www.who.int/iris/handle/10665/43811

Yahalom-Peri, T., Bogina, V., Basson-Shleymovich, Y., Azmon, M., Kuflik, T., Kodesh, E., Volpato, S., & Cukierman-Yaffe, T. (2023). Characterizing movement patterns of older individuals with t2d in free-living environments using wearable accelerometers. Journal of Clinical Medicine, 12(23). https://doi.org/10.3390/jcm12237404

Yan, Y., & Ou, Y. (2017). Accurate fall detection by nine-axis imu sensor. 2017 IEEE International Conference on Robotics and Biomimetics (ROBIO), 854–859. https://doi.org/10.1109/robio. 2017.8324524

Yu, X. (2008). Approaches and principles of fall detection for elderly and patient. HealthCom 200810th International Conference on e-health Networking, Applications and Services, 42–47. https://doi.org/10.1109/HEALTH.2008.4600107

Zeagler, C. (2017). Where to wear it: Functional , technical , and social considerations in on body location for wearable technology 20 years of designing for wearability. International Symposium on Wearable Computers., 150–157. https://doi.org/10.1145/3123021.3123042